Vibrational Modes of Tyrosines in Cytochrome c Oxidase from Paracoccus denitrificans : FTIR and Electrochemical Studies on Tyr-D 4 -labeled and on Tyr280His and Tyr35Phe Mutant Enz...

10 AUTHORS, INCLUDING:

Petra Hellwig
University of Strasbourg
143 PUBLICATIONS **2,277** CITATIONS

Robert B Gennis
University of Illinois, Urbana-Champaign
371 PUBLICATIONS **12,576** CITATIONS

Werner Mäntele
Goethe-Universität Frankfurt am Main
85 PUBLICATIONS **1,347** CITATIONS

Vibrational Modes of Tyrosines in Cytochrome *c* Oxidase from *Paracoccus denitrificans*: FTIR and Electrochemical Studies on Tyr-D4-labeled and on Tyr280His and Tyr35Phe Mutant Enzymes[†]

Petra Hellwig,*,[‡] Ute Pfitzner,[§] Julia Behr,[‖] Borries Rost,[‡] Russell P. Pesavento,[⊥] Wilfred v. Donk,[⊥] Robert B. Gennis,[#] Hartmut Michel,[‖] Bernd Ludwig,[§] and Werner Mäntele[‡]

Institut für Biophysik der Johann Wolfgang Goethe Universität, Theodor-Stern-Kai 7 Haus 74, 60590 Frankfurt/M., Germany, Institut für Biochemie der Johann Wolfgang Goethe Universität, Molekulare Genetik, Biozentrum, Marie-Curie-Strasse 9, 60439 Frankfurt/M., Germany, Max-Planck-Institut für Biophysik, Abteilung Molekulare Membranbiologie, Heinrich-Hoffmann-Strasse 7, 60528 Frankfurt/M., Germany, Department of Chemistry, University of Illinois, 600 South Mathews Avenue, Urbana, Illinois 61801, and Department of Biochemistry, University of Illinois, 600 South Mathews Avenue, Urbana, Illinois 61801

ABSTRACT: A combined electrochemical and FTIR spectroscopic approach was used to identify the vibrational modes of tyrosines in cytochrome *c* oxidase from *Paracoccus denitrificans* which change upon electron transfer and coupled proton transfer. Electrochemically induced FTIR difference spectra of the Tyr-D4-labeled cytochrome *c* oxidase reveal that only small contributions arise from the tyrosines. Contributions between 1600 and 1560 cm^{-1} are attributed to $\nu_{8a/8b}(CC)$ ring modes. The $\nu_{19}(CC)$ ring mode for the protonated form of tyrosines is proposed to absorb with an uncommonly small signal at 1525−1518 cm^{-1} and for the deprotonated form at 1496−1486 cm^{-1}, accompanied by the increase of the $\nu_{19}(CC)$ ring mode of the Tyr-D4-labeled oxidase at approximately 1434 cm^{-1}. A signal at 1270 cm^{-1} can be tentatively attributed to the $\nu_{7'a}(CO)$ and $\delta(COH)$ mode of a protonated tyrosine. Uncommon absorptions, like the mode at 1524 cm^{-1}, indicate the involvement of Tyr280 in the spectra. Tyr280 is a crucial residue close to the binuclear center and is covalently bonded to His276. The possible changes of the spectral properties are discussed together with the absorbance spectra of tyrosine bound to histidine. The vibrational modes of Tyr280 are further analyzed in combination with the mutation to histidine, which is assumed to abolish the covalent bonding. The electrochemically induced FTIR difference spectra of the Tyr280His mutant point to a change in protonation state in the environment of the binuclear center. Together with an observed decrease of a signal at 1736 cm^{-1}, previously assigned to Glu278, a possible functional coupling is reflected. In direct comparison to the FTIR difference spectra of the D4-labeled compound and comparing the spectra at pH 7 and 4.8, the protonation state of Tyr280 is discussed. Furthermore, a detailed analysis of the mutant is presented, the FTIR spectra of the CO adduct revealing a partial loss of Cu$_B$. Electrochemical redox titrations reflect a downshift of the heme a_3 midpoint potential by 95 ± 10 mV. Another tyrosine identified to show redox dependent changes upon electron transfer is Tyr35, a residue in the proposed D-pathway of the cytochrome *c* oxidase.

Cytochrome *c* oxidase is the terminal enzyme of the respiratory chain and catalyzes the stepwise reduction of oxygen to water. In the course of this process, electron and proton transfer are efficiently coupled to contribute to the formation of an electrochemical proton gradient, which drives ATP synthesis. (For recent reviews see refs *1* and *2*). Four redox-active cofactors are involved in electron transfer. Cu$_A$ acts as electron acceptor from cytochrome *c* and transfers the electron to heme *a*. Further electron transfer leads to the binuclear center, formed by heme a_3 and Cu$_B$, where oxygen is bound and reduced. Two putative proton pathways have been discussed. The K-pathway leads from the cytoplasm to the binuclear center through Ser191, Lys354, Thr351, and Tyr280 (the amino acid numbering in this paper refers to that of the *aa$_3$*-oxidase from *Paracoccus denitrificans* if not specifically mentioned). This pathway is discussed to be used for proton uptake coupled to the reduction of the heme a_3 Cu$_B$ site (*3*−*5*). In the Lys354 mutants, the turnover with O$_2$ is inhibited, whereas the enzyme is still active with H$_2$O$_2$ as an electron acceptor (*6*, *7*), suggesting that the protons involved in the oxidative part of the cycle follow a different path. The proposed D-pathway leads from Asp124, via polar residues, including Tyr35, to the highly conserved residue Glu278.

* To whom correspondence should be addressed. E-mail: hellwig@biophysik.uni-frankfurt.de. Phone: 49-69-6301-4227. Fax: 49-69-6301-5838.

‡ Institut für Biophysik der Johann Wolfgang Goethe Universität.
§ Institut für Biochemie der Johann Wolfgang Goethe Universität.
‖ Max-Planck-Institut für Biophysik.
⊥ Department of Chemistry, University of Illinois.
Department of Biochemistry, University of Illinois.

Tyr280 is a crucial amino acid close to the binuclear center. It is suggested to form a neutral tyrosine radical in the catalytic cycle and is a putative electron and/or proton donor (8−11). Electrostatic calculations indicate that in the oxidized enzyme Tyr280 is expected to be neutral when a negative ligand such as OH^- is bound in the binuclear center and deprotonated if not (12). On the basis of the structural data of the cytochrome *c* oxidase from bovine heart oxidase and from *P. denitrificans*, a covalent link between Tyr280 and His276 was found (8, 13), with both residues supposedly maintaining two separate π-electron systems (10). The cross-link could be verified by peptide analysis (14).

In previous work from our group, we have used sensitive FTIR[1] difference spectroscopy to study the reorganizations in the cytochrome *c* oxidase from *P. denitrificans* upon electron transfer and concomitant proton transfer (15−18, 40). In the approach presented here, we study a preparation of the cytochrome *c* oxidase from *P. denitrificans* in which all tyrosine residues have been replaced by ring-deuterated tyrosines, thus allowing the identification of the vibrational modes of tyrosines contributing to electrochemically induced FTIR difference spectra. Together with the FTIR difference spectra of the Tyr280His and the Tyr35Phe mutant enzymes, the protonation state of Tyr280 and Tyr35 as well as their interactions with the protein are characterized.

MATERIALS AND METHODS

Sample Preparation. Cytochrome *c* oxidase from *P. denitrificans* was prepared as described previously (19). D4-labeled tyrosine (Campro Scientific, Germany) was incorporated as previously described (20). The labeling rate of the preparation used here was found to exceed 60% as judged from the decrease of the signal intensity of the ν_{19}(C−C) tyrosine ring vibrational mode at 1518 cm^{-1} in the infrared absorbance spectra (data not shown) and 90% as reported in ref 20. Tyr280 was replaced by histidine by site-directed mutagenesis, resulting in an enzyme with a residual turnover activity of ∼1%. Tyr35 was changed to phenylalanine, resulting in a decrease of the activity to 60% but a H$^+$/e$^-$ ratio close to that of the wild-type. For experimental details see refs 5, 19, and 21.

The CO adduct of cytochrome *c* oxidase was prepared by reduction with a phosphate-buffered $Na_2S_2O_4$ solution (pH 7), followed by incubation with CO gas. (For details, see ref 22.) A total of 3−4 μL of the sample were used to fill an infrared cell consisting of two CaF$_2$ windows with a path length of 15 μm.

For electrochemistry, the protein samples were concentrated to approximately 0.5 mM using Microcon ultrafiltration cells (Millipore, Bedford, MA), 200 mM phosphate buffer (pH 7) or in 200 mM cacodylate buffer (pH 4.8), both containing 100 mM KCl and 0.1% *n*-decyl-β-D-maltopyranoside. At a pH of 4.5, an activity of 250 s^{-1} was observed for wild-type cytochrome *c* oxidase from *P. denitrificans* (23).

Absorption spectra of free tyrosine and of the Tyr-His model compound (*c* ∼ 20 mM) were recorded in HCl (1 M) or NaOH (1 M) in a cell consisting of two CaF$_2$ windows

with a path length of 7.8 μm; 0.6 μL of the sample were sufficient to fill the cell. The Tyr-His model compound, 2-imidazole-1-yl-4-methylphenol, was previously reported in ref 41.

Electrochemistry. The ultrathin layer spectroelectrochemical cell for the UV−vis and IR was used as previously described (24). Sufficient transmission in the 1800−1000 cm^{-1} range, even in the region of strong water absorbance around 1645 cm^{-1}, was achieved with the cell path length set to 6−8 μm. The gold grid working electrode was chemically modified with a 2 mM cysteamine solution as reported before (16). To accelerate the redox reaction, 16 different mediators were added as reported in ref 16 (except *N*-methylphenazoniummethosulfate and *N*-ethylphenazoniumsulfate, but including neutral red; E_m: −307 mV vs SHE′) to a final concentration of 45 μM each. At this concentration, and with the cell path length below 10 μm, no spectral contributions from the mediators in the visible and IR range could be detected in control experiments with samples lacking the protein, except for the PO modes of the phosphate buffer between 1200 and 1000 cm^{-1}. For the electrochemical titrations, 15 μM horse heart cytochrome *c* was added as mediator. Potentials quoted with the data refer to the Ag/AgCl/3 M KCl reference electrode; add +208 mV for SHE′ (pH 7) potentials.

The UV−vis redox titrations were performed by stepwise setting the potential steps and recording the spectrum after equilibration. Typically, data were recorded at steps of 50 mV. The midpoint potentials E_m and the number n of transferred electrons were obtained by adjusting a calculated Nernst curve to the measured absorbance change at a single wavelength by an interactive fit as previously described in Hellwig et al. (18).

Spectroscopy. FTIR and UV−vis difference spectra as a function of the applied potential were obtained simultaneously from the same sample with a setup combining an IR beam from the interferometer (modified IFS 25, Bruker, Germany) for the 4000−1000 cm^{-1} range and a dispersive spectrometer for the 400−900 nm range. Electrochemically induced difference spectra were recorded and processed as previously described in Hellwig et al. (16).

The difference spectra of CO rebinding to the fully reduced cytochrome *c* oxidase were induced with a frequency doubled Nd:YAG laser (Spectron Laser Systems SL454G) and recorded with a modified FTIR spectrometer in the rapid scan mode (IFS-66, Bruker, Germany). Data were collected and processed as reported in ref 22.

RESULTS AND DISCUSSION

D4-Labeled Tyrosines

Absorbance Spectra of Tyrosines in Solution. Figure 1 shows the absorbance spectra of unlabeled (A) and D4-labeled (B) tyrosine in HCl solution (1 M) and of unlabeled (C) and D4-labeled (D) tyrosine in NaOH solution (1 M). The contributions of the solvent were subtracted. The signals at 1539, 1455, and 1291 cm^{-1} arise from the vibrations of the tyrosine β-methylene group (25) and are insensitive to isotope substitutions at the phenol ring. The overlap by other modes, however, may lead to variations in the peak frequencies. The signals at 1615 and 1599 cm^{-1} in the spectra of the protonated tyrosine (Figure 1A) can be attributed to the
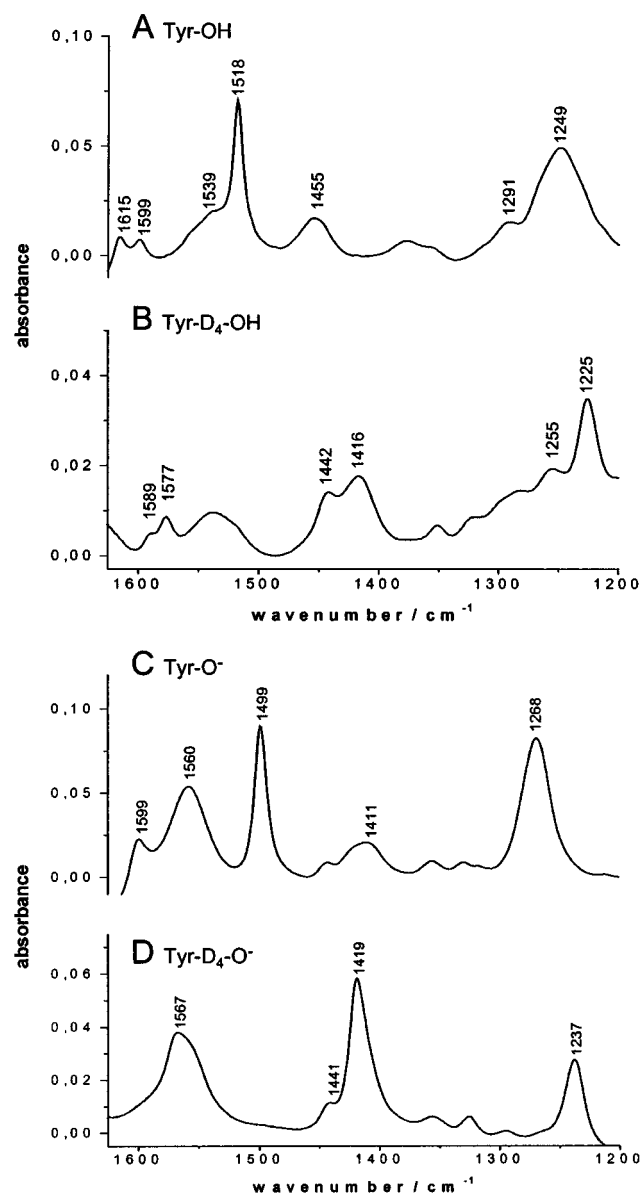

FIGURE 1: Absorbance spectra of unlabeled and D₄-labeled tyrosine in situ protonated upon solution in 1 M HCl (A, B) and deprotonated upon in 1 M NaOH (C, D). The contributions of the solvent were interactively subtracted. The arrows indicate the shifts by the D₄-labeling.
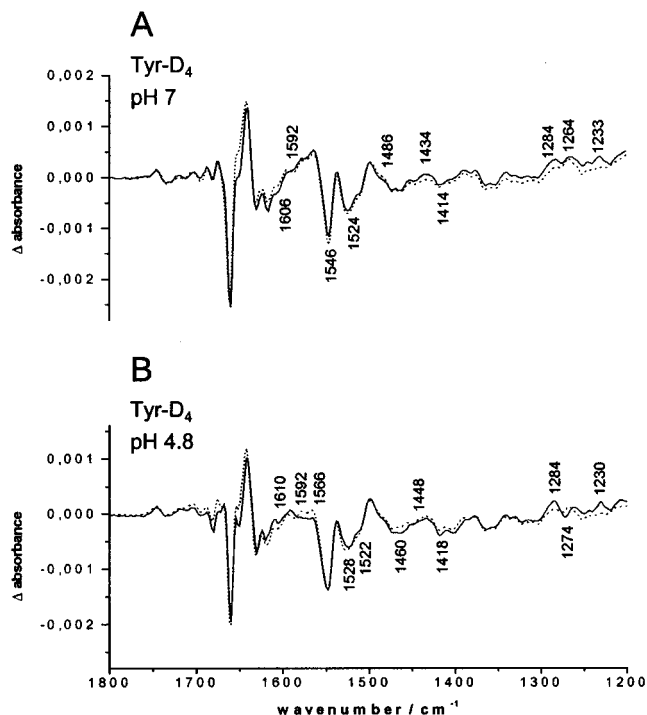

FIGURE 2: Oxidized-minus-reduced FTIR difference spectra of wild-type (dotted line) and Tyr-D₄-labeled cytochrome *c* oxidase (solid line) for a potential step from −0.5 to 0.5 V in the spectral range from 1800 to 1200 cm⁻¹ at pH 7 (A) and at pH 4.8 (B).

ring ν_{8a} and ν_{8b}(CC) modes and the signal at 1518 cm⁻¹ to the ν_{19}(CC) ring mode. At 1249 cm⁻¹, a signal composed of the $\nu_{7'a}$(CO) vibration and the δ(COH) vibration can be seen. Upon D₄-labeling at the ring (Figure 1B), shifts of the $\nu_{8a/8b}$(CC) ring modes to 1589 and 1577 cm⁻¹ and of the ν_{19}-(CC) ring mode to a split signal at 1442 and 1416 cm⁻¹ occur. The overlapping $\nu_{7'a}$(CO) and δ(COH) vibrations can be seen at 1225 cm⁻¹. These assignments are in accordance with previous band attributions (*26*), except for small shifts of 1−2 cm⁻¹ that can be attributed to differences in spectral resolution.

For deprotonated tyrosine in solution (Figure 1C), the $\nu_{8a/8b}$(CC) ring modes can be identified at 1599 and 1560 cm⁻¹ and the ν_{19}(CC) ring mode at 1499 cm⁻¹, thus reflecting the sensitivity of the ring modes to the protonation state of the phenol group. The $\nu_{7'a}$(CO) mode is present at 1269 cm⁻¹. Upon D₄-labeling, a downshift of the ν_{8a} (CC) ring mode to

1567 cm⁻¹, of the ν_{19}(CC) ring mode to 1419 cm⁻¹, and of the $\nu_{7'a}$(CO) mode to 1237 cm⁻¹ can be seen.

Electrochemically Induced FTIR Difference Spectra of the Enzyme Containing Ring-Deuterated Tyrosine. To identify the vibrational modes of tyrosines in the electrochemically induced FTIR difference spectra of the cytochrome *c* oxidase, the enzyme with ring D₄-labeled tyrosines was used (for details, see Materials and Methods and ref *20*). Figure 2 shows the electrochemically induced FTIR difference spectra of cytochrome *c* oxidase from *P. denitrificans* for a potential step from −0.5 to 0.5 V at pH 7 (A) and pH 4.8 (B). For the following discussion, we keep in mind that the labeling rate was determined to exceed 60% on the basis of the decrease of the mode at 1518 cm⁻¹ in the infrared absorption spectra and that the signals concomitant with the tyrosines thus may not be fully shifted.

In the electrochemically induced FTIR difference spectra for pH 7 (Figure 2A), only small shifts upon D₄-labeling can be observed. The small variations between 1600 and 1560 cm⁻¹ reflect the shifts of the $\nu_{8a/8b}$(CC) ring modes upon D₄-labeling as observed before for the tyrosines in solution (Figure 1A−D). In detail, the variation of a signal at 1584 cm⁻¹ is accompanied by the change of a signal at 1592 cm⁻¹ and further small variations between 1610 and 1600 cm⁻¹ can be seen. In the spectral region characteristic for the ν_{19}(CC) ring mode of the protonated form at approximately 1518 cm⁻¹ and at 1496−1486 cm⁻¹ for the deprotonated form, only very small variations are accompanied by the increase of the modes of the ν_{19}(CC) ring mode of the Tyr-D₄-labeled oxidase at approximately 1434 cm⁻¹. In the spectral range from 1530 to 1546 cm⁻¹, small shifts in intensity are observable that cannot be correlated with known tyrosine modes (cf. Figure 1). Because all shifts observed here can be related to the labeling of tyrosines, we

have to assume that the tyrosines involved in the redox reaction exhibit uncommon spectroscopic properties.

Between 1300 and 1200 cm^{-1}, the decrease of the $\nu_{7'a}$(CO) and δ(COH) at 1266 cm^{-1} and the increase of signals for the Tyr-D$_4$-labeled form at 1284 and 1233 cm^{-1} (cf. Figure 1B,D) is evident. The signals could arise from both the protonated or the deprotonated form, because an influence of the hydrogen bonding to/from the observed tyrosine on the modes can be expected and the position of the $\nu_{7'a}$(CO) mode may thus strongly differ from tyrosines in solution presented in Figure 1. The signal at approximately 1280 cm^{-1}, in the Tyr-D$_4$-labeled form, is significantly more intense as compared with that in the spectra of the D$_4$-labeled tyrosines in solution (cf. Figure 1B,D), suggesting the presence of a tyrosine residue with perturbed vibrational modes.

On the basis of the data presented for pH 7 (Figure 2A), the protonation/deprotonation of a tyrosine upon oxidation/ reduction of the enzyme can be excluded because the shifted signals observed here are significantly smaller than expected on the basis of the extinction coefficient of the tyrosines in solution (cf. Figure 1). It is rather possible that the difference signals observed here are caused by small changes of the extinction coefficient upon the environmental changes concomitant with the electron transfer and coupled processes. However, it is not clear if the tyrosine residues that can be seen in the electrochemically induced FTIR difference spectra are fully protonated, because some of the difference signals do not match those known from unperturbed tyrosines. We have thus studied the electrochemically induced FTIR difference spectra at pH 4.8, where full protonation can be expected (Figure 2B). The cytochrome *c* oxidase from *P. denitrificans* shows fully reversible redox reactions at pH 4.8. The difference spectra of the unlabeled enzyme (dotted line) at pH 7 (Figure 2A) and at pH 4.8 (Figure 2B) exhibit significant pH-depended alterations such as the decrease of the signals at 1592 and 1528 cm^{-1}, the shift of the signal at 1672 cm^{-1} and at 1746 cm^{-1}, the latter described in ref *16*. These variations occur in spectral ranges characteristic for protonated or deprotonated aspartic acid and glutamic acid side chain groups as well as for heme propionates and thus point to protonation changes. In addition, the variations in the spectra at different pH values may be explained by environmental changes in the protein. The differences in the protein at different pH values have been previously revealed in the structure for pH 7 and 5.5, where a different distance between Cu$_B$ and Tyr280 was reported (*8*).

The spectra of the Tyr-D$_4$-labeled cytochrome *c* oxidase at pH 4.8 (Figure 2B) show clear differences as compared to those at pH 7 and are shown in an enlarged view in Figure 3A as well as a double difference spectrum. The decrease of a signal at 1578 and 1566 cm^{-1} was not observed in the spectra for the Tyr-D$_4$-labeled cytochrome *c* oxidase at pH 7; thus, at the lower pH value, different alterations of the $\nu_{8a/8b}$(CC) ring modes upon D$_4$-labeling of the tyrosines can be seen. The shift from 1588 to 1592 cm^{-1} is similar to that at pH 7. In the spectral range characteristic for the ν_{19}(CC) ring mode, signals are decreased at 1528 and 1516 cm^{-1}, and the signal that can be observed at 1528 cm^{-1} for the wild-type enzyme is shifted to 1522 cm^{-1}. The modes at 1486−1496 cm^{-1}, changed upon D$_4$-labeling at pH 7, are not observed anymore and a new signal at 1460 cm^{-1} is
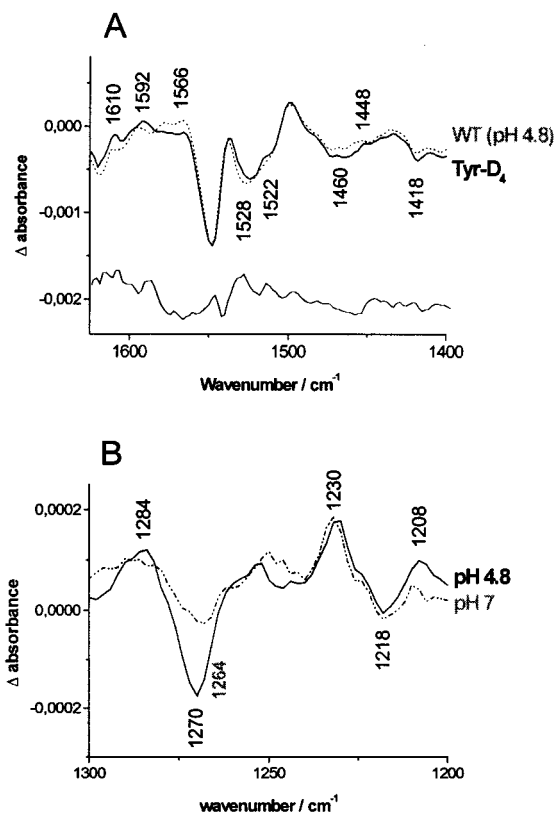

FIGURE 3: Enlarged view of the oxidized-minus-reduced FTIR difference spectra for pH 4.8 (Figure 2) from 1625−1400 cm^{-1} and double difference spectrum (A). Double difference spectra obtained by subtraction of the spectra of the wild-type and Tyr-D$_4$-labeled cytochrome *c* oxidase for pH 7 (dotted-dotted line) and pH 4.8 (full line) (B) from 1300−1200 cm^{-1}.

evident. The ν_{19}(CC) ring mode of the Tyr-D$_4$-labeled oxidase is still present at 1430 cm^{-1}. The strongest variation occurs between 1300 and 1200 cm^{-1} where the difference signal at approximately 1268 cm^{-1} is completely lost in the spectra at pH 4.8 upon D$_4$-labeling, in contrast to the data at pH 7. The signal at 1284 cm^{-1} is more intense for pH 4.8 as well. The changes in this spectral range can be seen in the double difference spectra shown in Figure 3B for pH 7 (dashed line) and pH 4.8 (solid line). The spectra were calculated by subtracting the spectra of the D$_4$-labeled enzyme from the wild-type spectra. The signal at 1270 cm^{-1}, clearly distinguishable in the double difference spectra, may be tentatively attributed to the $\nu_{7'a}$(CO) and δ(COH) modes of a protonated tyrosine, based on the observations of the pH dependency of this signal.

The electrochemically induced FTIR difference spectra of the Tyr-D$_4$-labeled cytochrome *c* oxidase allow for the identification of tyrosine vibrational modes. Furthermore, these modes clearly differ between acidic and neutral pH, thus raising the question whether the difference spectra reflect the protonation of a tyrosine residue or whether strong variations of the extinction coefficient(s) caused by changes of the environment of a specific tyrosine residue with pH might explain the observed spectra. For the tyrosines in the cytochrome *c* oxidase, full protonation at pH 7 has been proposed on the basis of electrostatic calculations (*12*). As described in the introduction, Tyr280 is discussed to be protonated if OH$^-$ is present in the binuclear center and deprotonated if not. Tyr280 is a crucial amino acid close to
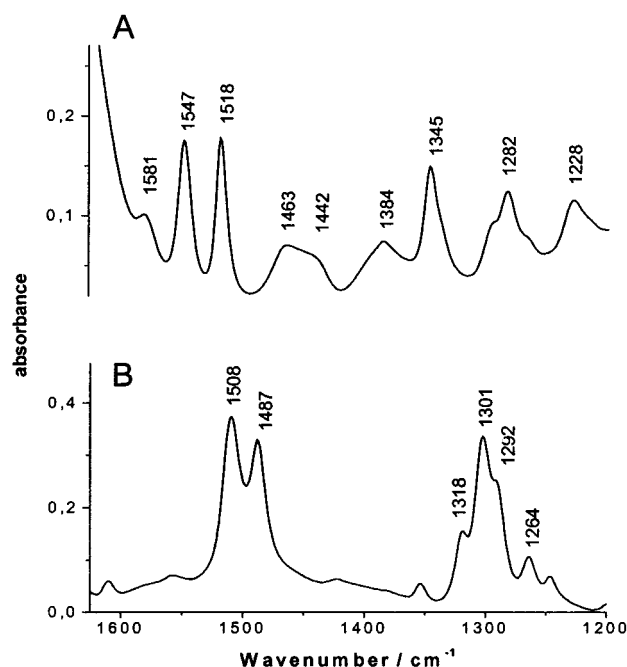
FIGURE 4: Absorbance spectra of model for tyrosine linked to a histidine; 2-imidazole-1-yl-4-methylphenol as previously reported in ref *41* in situ protonated upon solution in 1 M HCl (A) and deprotonated upon in 1 M NaOH (B).
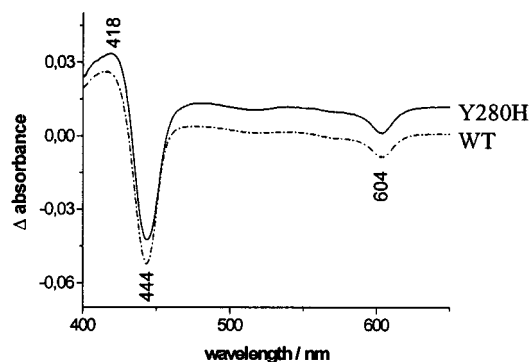

FIGURE 5: Oxidized-minus-reduced UV−vis difference spectra of wild-type and Tyr280His mutant cytochrome *c* oxidase from *P. denitrificans* obtained for a potential step from −0.5 to 0.5 V (vs Ag/AgCl/3 M KCl).

the binuclear center (see introduction) and covalently linked to His276, with both residues presumably keeping their individual π-electron systems. The bonding at the tyrosine ring reduces the symmetry of the ring and accordingly influences its vibrational modes.

Absorbance Spectra of a Model for Tyrosine Bound to Histidine. To elucidate possible differences in the vibrational modes of this linked tyrosine, a model compound, 2-imidazole-1-yl-4-methylphenol, previously introduced in ref *41*, was studied. Figure 4 shows the absorbance spectrum of the compound at the same conditions as the free tyrosine spectra shown in Figure 1. At a pH value of 2 (Figure 4A), both the imidazole as well as the phenol site are protonated, while at a pH value of 12 (Figure 4B) the deprotonated and neutral form, respectively, can be expected. Histidine in solution shows contributions with an extinction coefficient below 90 $M^{-1} cm^{-1}$, except for the $\nu(C=C)$ mode of protonated histidines at 1633 cm^{-1} (*26*). On this basis, an equimolar mix of tyrosine with histidine measured at the same pH conditions as the His-Tyr model leads to a spectrum which is comparable to the one presented in Figure 1A and C, respectively.

The data clearly demonstrate that the linkage causes changes in the spectral properties; several additional modes are observable. The $\nu_{19}(CC)$ ring mode of the protonated tyrosine, which exhibits a sharp mode at approximately 1518 cm^{-1}, is still present; however, a new strong mode at 1547 cm^{-1} appears. This is in line with the variation between 1525 and 1518 cm^{-1} seen in Figure 2B for the protein. Strong variations are observable between 1360 and 1230 cm^{-1} in comparison to Figure 1. The contributions for the deprotonated form of the vibration is split from 1499 cm^{-1} to signals at 1508 and 1487 cm^{-1}. The $\nu_{7'a}(CO)$ and $\delta(COH)$ modes seem to shift from 1268 to 1301 cm^{-1}.

This clearly shows that the linkage strongly changes spectral properties of a tyrosine; thus, Tyr280 will not show

"normal" tyrosine contributions. A more detailed analysis of the shifted modes, however, remains difficult without labeling experiments. We also keep in mind that the imidazole ring may change its spectral properties due to the linkage and could thus be involved in the spectra.

Tyrosine Mutants

While the electrochemically induced FTIR difference spectra of the Tyr-D_4-labeled cytochrome *c* oxidase reveal contributions of all tyrosines reorganizing upon electron transfer, a further attribution to individual tyrosines requires analysis of site-directed mutants. The most critical tyrosine, Tyr280, was probed by analysis of the Tyr280His mutant enzyme. Furthermore, the Tyr35Phe and Tyr406Phe mutants were studied. The first two mutants lead to substantial alterations in the IR difference spectra, which are discussed below. The Tyr406Phe mutant enzyme, however, showed a strongly shifted α band in the visible and shifted heme contributions in the infrared (*17*). No mode correlating with the signals affected by Tyr-D_4-labeling was shifted; this mutant will thus not be discussed here.

Tyr280His

In the Tyr280His mutant, the covalent bond to His276 is assumed to be missing. To judge the distortion of the binuclear center upon this strong structural impact, the mutant was characterized by UV−vis spectroscopy, electrochemical potential titrations, and FTIR spectroscopy on the CO adduct.

UV−vis Difference Spectra of Tyr280His. Figure 5 shows the oxidized-minus-reduced UV−vis difference spectra of wild-type and Tyr280His mutant cytochrome *c* oxidase from *P. denitrificans* obtained for a potential step from −0.5 to 0.5 V (vs Ag/AgCl/3 M KCl). The positive difference signals correlate with the oxidized and the negative signals with the reduced forms of the enzyme. The α band and the Soret band are only shifted by about 1−3 nm. In contrast to the Tyr280 mutant enzymes reported for other organisms (*27−29*), the influence on the UV−vis spectra is negligible and the perturbation of the hemes seems to be extremely low.

FTIR Difference Spectra of the CO Adduct from Tyr280His. At cryogenic temperatures, CO photolytically dissociates from CO-poisoned heme a_3 and remains bound to Cu_B (*30*). The low-temperature FTIR difference spectra of the CO adduct were thus used to quantify the amount of Cu_B and to investigate the possible distortion of the protein site around
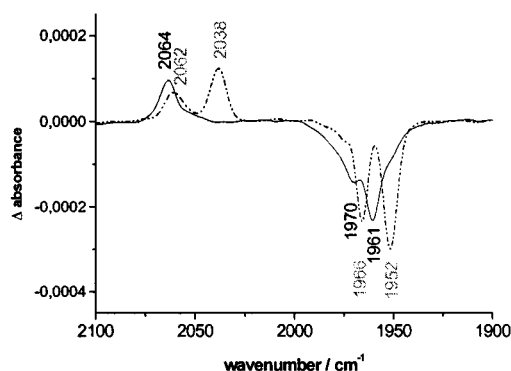
FIGURE 6: CO modes of the fully reduced wild-type (dotted line) and Tyr280His mutant (solid line) cytochrome *c* oxidase in the light-minus-dark FTIR difference spectra at 84 K.

the binuclear center as previously shown in refs *3* and *27*. In Figure 6, the light-minus-dark difference spectra at 84 K of the wild-type (dotted line) and the Tyr280His mutant cytochrome *c* oxidase (solid line) can be seen. The stretching frequencies of CO bound to heme a_3 of the wild-type enzyme can be found at 1966 and 1952 cm^{-1}, shifted to 1970 and 1961 cm^{-1} for the Tyr280His mutant enzyme. The stretching frequency of CO bound to Cu$_B$ can be seen at 2062 and at 2038 cm^{-1} for the wild-type and at 2064 cm^{-1} with a shoulder at 2054 cm^{-1} for the Tyr280His mutant enzyme.

The CO bound to fully reduced cytochrome *c* oxidase exhibits two conformations, termed α and β form. They have been previously reported for the aa_3-oxidase from *R. sphaeroides* (*31, 32*) and were recently identified for the aa_3-oxidase from *P. denitrificans* (*22*). The signals at 1966/2062 cm^{-1} were assigned to the α form and the signals at 1952/2038 cm^{-1} to the β form of the wild-type cytochrome *c* oxidase from *P. denitrificans* (*22*). In the Tyr280His mutant enzyme (Figure 6), the position of the CO mode is shifted to higher wavenumbers. The shifts of the CO stretching modes visualize the distortion in the binding pocket induced by the mutation.

The presence of a positive signal at 2064 cm^{-1} indicates the presence of Cu$_B$ in the binuclear center of the Tyr280His mutant enzyme. However, the ratio of the intensity for the stretching mode of CO bound to heme a_3 and to Cu, respectively, is modified. According to Thomas et al. (*27*), the rebinding of CO to the heme a_3 center, in the case of Cu$_B$ loss, can be monitored for temperatures up to 100 K and, thus, the spectra displayed may include contributions of centers with partial Cu$_B$ loss. Assuming that the extinction coefficient of the Cu$_B$−CO and the heme a_3−CO mode is unaffected by the changes in the mutant enzyme, a loss of Cu$_B$ of about 50% could be estimated. Certainly, the strong variations in the protein structure and the resulting environmental changes influence the extinction coefficients. Additionally an influence of the mutation on the temperature dependence of the conformers of the CO modes, which was previously reported for the cytochrome *c* oxidase from *P. denitrificans*, is possible (*22*).

In a previous publication, Tyr280 mutants in cytochrome bo_3 from *Escherichia coli* were studied with an analogous IR spectroscopic approach, revealing the complete loss of Cu$_B$ and proposing Tyr280 to be an essential element forming the Cu$_B$ site (*27*).
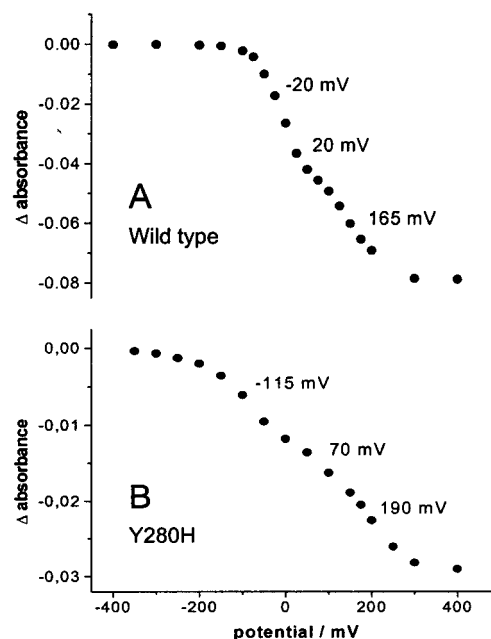

FIGURE 7: Oxidative redox titration of the Soret-band from wild-type (A) and Tyr280His (B) mutant cytochrome *c* oxidase at 444 nm. The data were interactively fitted to a calculated Nernst curve. Three midpoint potentials can be determined from these fits: $E_{m1} = -0.02 \pm 0.01$ V, $E_{m2} = 0.02 \pm 0.02$ V, and $E_{m3} = 0.165 \pm 0.03$ V for wild-type and $E_{m1} = -0.115 \pm 0.02$ V, $E_{m2} = 0.07 \pm 0.02$ V, and $E_{m3} = 0.190 \pm 0.03$ V for the Tyr280His mutant. Different concentrations were used.

Redox Titrations of Tyr280His. Figure 7 presents the potential dependent development of the Soret band from wild-type (A) and Tyr280His mutant cytochrome *c* oxidase (B) at 444 nm. The Nernst fit yielded three midpoint potentials: $E_{m1} = -0.02 \pm 0.01$ V, $E_{m2} = 0.02 \pm 0.02$ V, and $E_{m3} = 0.165 \pm 0.03$ V for wild-type and $E_{m1} = -0.115 \pm 0.02$ V, $E_{m2} = 0.07 \pm 0.02$ V, and $E_{m3} = 0.190 \pm 0.03$ V for the Tyr280His mutant. The number of transferred electrons *n*, left as an open variable in the fit (cf. ref *18*), was determined to be 0.8−1 for each step. A triphasic titration curve can be seen for the wild-type enzyme. In previous work, the potentials of the heme centers in the cytochrome *c* oxidase from bovine heart have been reported to be indistinguishable in the absence of inhibitors due to their cooperativity and to the cooperativity with Cu$_B$ (*33*−*38*). A triphasic titration curve describing the cooperative interactions of the hemes and Cu$_B$ and with both hemes contributing to the phases is expected. The potential dependent development of the contributions in the UV−vis is first dominated by heme a_3 and then by the heme a contributions. For the analysis of the complex data originating from the cooperative interactions between the redox centers, several models have been developed. The most prominent one is the neoclassical model (*33*). In a previous work, we have presented the titration curve of the wild-type enzyme for the cytochrome *c* oxidase from *P. denitrificans* for the particular purpose to separate the two potential steps and to obtain the contributions of the hemes a and a_3 (*18*). The second step of the titration curve, observed at 0.02 V (Figure 7A), was not discussed there, being less clear than in the titration curves of the bovine heart oxidase (*33*−*38*). This discrepancy may be attributed to slightly different
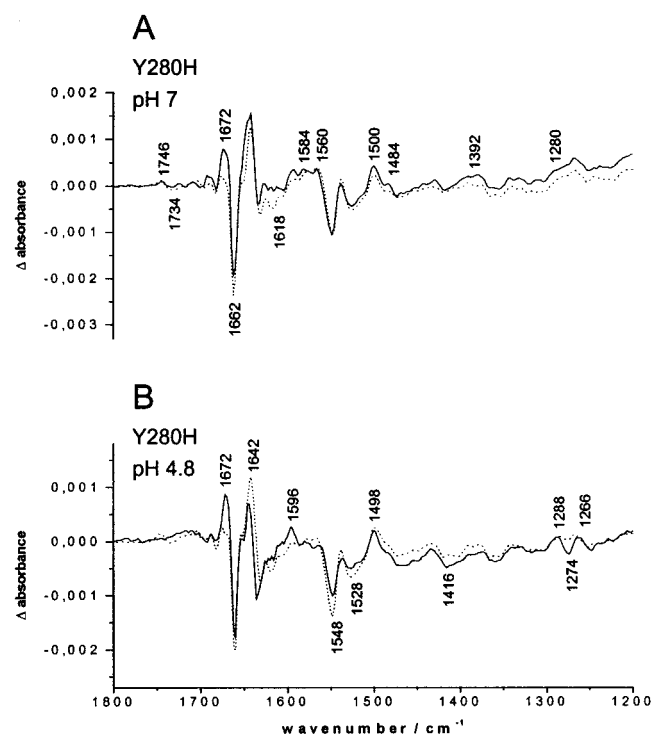
A

B

FIGURE 8: Oxidized-minus-reduced FTIR difference spectra of wild-type (dashed line) and Tyr280His mutant (solid line) cytochrome *c* oxidase from *P. denitrificans* obtained for a potential step from -0.5 to 0.5 V (vs Ag/AgCl/3 M KCl) at pH 7 (A) and at pH 4.8 (B).

cooperativity between the redox centers. In addition to that, differences in the extinction coefficient of the hemes, present among different organisms, influence the relative intensity of the different steps.

The titration curves from the Tyr280His mutant enzyme (Figure 7B) reflect a 95 mV ($\pm$20mV) downshift of the potential in a region where heme a_3 dominates (*18*). A reasonable interpretation of this shift is in terms of substantial structural changes in the environment of heme a_3 upon the mutation, which will be discussed on the basis of the FTIR difference spectra (Figure 8). Das et al. (*28*) proposed a shift of the heme a_3 potential on the basis of UV−vis data for the Tyr280Phe mutant enzyme in aa_3-oxidase from *R. sphaeroides*. This shift could be found here with potential titrations for the Tyr280His aa_3-oxidase from *P. denitrificans*. In addition, shifts of the second and third potential step can be observed reflecting the changes in the system. Because Cu$_B$ cooperativity with the hemes causes the observed triphasic titration curve (*33, 36*), the presence of Cu$_B$ may be deduced from the titration curves.

Electrochemically Induced FTIR Difference Spectra of the Tyr280His Mutant Enzyme. Figure 8A shows the oxidized-minus-reduced FTIR difference spectra of wild-type (dotted line) and Tyr280His mutant enzyme (solid line) for a potential step from -0.5 to 0.5 V in the spectral range from 1800 to 1200 cm^{-1} at pH 7. The electrochemically induced FTIR difference spectra of the cytochrome *c* oxidase from *P. denitrificans* have been examined in detail in Hellwig et al. (*15, 16, 18*) and in Behr et al. (*17, 40*). The changes in the difference spectra of the Tyr280His mutant are discussed on the basis of these previous assignments.

In the spectra of the Tyr280His mutant, the negative difference signal at 1734 cm^{-1} is clearly decreased (figure

8A). This mode was previously assigned to the ν(C=O) mode of the protonated side chain of Glu278 (*15, 16*), coupled to the redox transition of the binuclear center (*18*). However, the signal at 1746/1734 cm^{-1}, attributed to a change of the Glu 278 environment coupled to the electron transfer to/from heme *a*, is unaffected (*16*). A strong increase of the difference signal at 1672 cm^{-1} is evident: a signal which was previously described to be composed of the ν-(C=O) mode from protonated heme propionates (*17*) and the formyl substituent of heme a_3 (*18*). An alternative contribution from the ν(C=O) modes of the polypeptide backbone can be discussed for this signal and for the small variations in position and intensity between 1660 and 1630 cm^{-1}. At 1618 cm^{-1}, the decrease of a negative band is observable. This band was tentatively assigned to the ν(C=C) mode of the vinyl group at the hemes (*18*). The changes at 1584, 1570, and 1560 cm^{-1} occur in the spectral region characteristic for deprotonated aspartic acid and glutamic acid side chains and heme propionates; the ν(COO$^-$)^{as} vibrational mode of deprotonated heme propionates was assigned before by specific ^{13}C labeling (*17*) to signals at 1570 and 1538 cm^{-1}. Further variations between wild-type and mutant enzyme from 1520 to 1200 cm^{-1} can be seen and may partially be attributed to Tyr280 or to structural variations caused by the mutation.

Figure 8B shows the electrochemically induced FTIR difference spectra for the Tyr280His mutant and the wild-type enzyme at pH 4.8. The signal at 1746/1734 cm^{-1}, previously assigned to Glu278, is absent, and further strong variations in position and intensity in the spectral range between 1710 and 1500 cm^{-1} are evident. The decrease of a signal in the spectral region at approximately 1268 cm^{-1} can be seen. The change in intensity of this signal is analogous to the change at pH 4.8 in the electrochemically induced FTIR difference spectra of the Tyr-D$_4$-labeled enzyme, allowing the assignment of the mode at 1268 cm^{-1} to the $\nu_{7'a}$(CO) and δ(COH) of protonated Tyr280.

Signals perturbed in both electrochemically induced FTIR difference spectra from the Tyr-D$_4$-labeled and the Tyr280 mutant enzyme are summarized for the following discussion in Table 1.

Is Tyr280 Protonated? The changes in the electrochemically induced FTIR difference spectra of the Tyr280His mutant enzyme reflect the strong structural perturbation in the enzyme caused by the loss of the covalent bond between Tyr280 and His276. In the FTIR spectra of the CO adduct (Figure 6), the partial presence of Cu$_B$ was shown. Modes reflecting the reorganizations of the protein upon electron transfer and coupled proton transfer to/from Cu$_B$ will thus be altered in the electrochemically induced FTIR difference spectra of the Tyr280His mutant (Figure 8).

The perturbation of the heme porphyrin ring modes, like the mode at 1546 cm^{-1}, (ν_{38y} mode; cf. ref *18*) is rather small. More prominent are the variations in the characteristic spectral range of protonated (1760−1700 cm^{-1}) and deprotonated (1590−1540 cm^{-1}) carboxyl groups, indicating a partial change in the protonation state of the Glu278 and the heme propionates and visualizing a change of the "local pK_A" values. The change of the protonation state in the protein environment of the binuclear center in the Tyr280His mutant can be interpreted in different ways. A functional

Table 1: Discussed Tyrosine Modes (in cm^{-1}) as Depicted from the Electrochemically Induced FTIR Difference Spectra of Wild-Type (WT), Tyr-D$_4$ Marked, and Tyr280His Mutant Cytochrome *c* Oxidase[a]

pH 7			pH 5			tentative assignments
WT	Tyr-D$_4$	Tyr280His	WT	Tyr-D$_4$	Tyr280His	
1616	1616	1622/1616	1618	1620	1616	
1606	1606	1604	1608	1602	1604	
1594		1592	1594		1596	
1588	1592	1584	1586	1592	1586	$\nu_{8a/8b}$(CC) Tyr ring
1578			1578	1574	1580	$\nu_{8a/8b}$(CC) Tyr ring
1564			1566	1566	1564	$\nu_{8a/8b}$(CC) Tyr ring
1524	1524	1526	1528	1522	1528	ν_{19}(CC) Tyr ring
1510	1508	1510	1510	1510	1518	ν_{19}(CC) Tyr ring
1482	1486	1484	1482		1484	
1462			1472	1472	1474	
			1464	1464/1460	1464	
			1452	1448	1450	
1434	1434	1428	1436	1432	1434	ν_{19}(CC) Tyr-D$_4$ ring
1420	1414	1418	1418	1420	1416	ν_{19}(CC) Tyr-D$_4$ ring
1388	1388	1392	1388	1386	1390	
1378		1378	1378	1378	1376	
1360			1366	1364	1366/1360	
1340		1344	1340	1340	1340	
1284	1280	1290/1280	1284	1284	1288	$\nu_{7'a}$(CO)/δ(OH) Tyr
1276	1276		1274	1272	1274	
1268	1264	1268	1268	1262	1260	$\nu_{7'a}$(CO)/δ(OH) Tyr
1250			1252	1248	1248	
1244	1244	1246	1244			
	1233			1230		$\nu_{7'a}$(CO)/δ(OH) Tyr-D$_4$
	1218			1220/1208		$\nu_{7'a}$(CO)/δ(OH) Tyr-D$_4$

[a] Only signals changing in intensity or frequency in the different experiments are shown. The tentative assignments suggested are based on model compound studies. For details, see text.

coupling between Glu278 and Tyr280 is possible, which is abolished in the mutant enzyme. Alternatively, the change of the protonation states may be a result of the structural changes caused by the mutation.

For the Tyr280Phe mutants from the cytochrome *c* oxidase from *R. sphaeroides* and the cytochrome *bo*$_3$ ubiquinol oxidase from *E. coli*, a strong perturbation of the hemes and the loss of Cu$_B$ were suggested (*28, 29*). A strong perturbation was also reported for the Tyr280His mutant cytochrome *bo*$_3$ ubiquinol oxidase from *E. coli* (*27*). A different effect of the mutation at Tyr280 can be reported for the cytochrome *c* oxidase from *P. denitrificans*. Discrepancies between the effect of site-directed mutations of crucial groups in different organisms such as *P. denitrificans* and *E. coli* were reported before, for example, in ref *5*, and show small differences in the protein environment.

The variations of the signal at 1270/1268 cm^{-1} at different pH values (cf. Table 1) that can be attributed to Tyr280 on the basis of the electrochemically induced FTIR difference spectra of the Tyr-D$_4$-labeled cytochrome *c* oxidase and the Tyr280His mutant enzyme may be interpreted in two different ways. The signal at 1268 cm^{-1} (cf. Figures 2A,B and 3B) may reflect a pH dependent change in extinction coefficient upon variations in the direct environment close to the Tyr280 residue. Alternatively, however, there may be a change of protonation state of Tyr280.

Tyr35Phe

Another interesting tyrosine in the cytochrome *c* oxidase from *P. denitrificans* is Tyr35, located in the discussed D-pathway and presumed to be a part of the interacting groups during proton transfer. The Tyr35Phe mutant enzyme retains ~60% electron transfer and full proton pump activity

(*5*). The electrochemically induced FTIR difference spectra are used to identify the interactions and reorganizations of this residue upon electron transfer and coupled proton-transfer reactions. Figure 9 presents the oxidized-minus-reduced FTIR difference spectra of the Tyr35Phe mutant enzyme for a potential step from −0.5 to 0.5 V at pH 7 (A) and at pH 4.8 (B).

In the spectral range from 1750 to 1700 cm^{-1}, no change in the electrochemically induced FTIR difference spectra can be seen comparing the wild-type spectra with the Tyr35Phe mutant enzyme. Between 1680 and 1620 cm^{-1}, changes in intensity of signals at 1678 and 1624 cm^{-1} can be observed. Signals in this spectral range were previously attributed to the perturbation of β-sheet secondary structure elements, or arising from the hemes *a* and *a*$_3$ (ν(C=O) modes of the formyl substituent and protonated heme propionates can be expected in this spectral range), or to arginine side chains (for assignments, see ref *18*). Because a mutation at Tyr35 is highly unlikely to perturb these residues, this interpretation can be ruled out. The variations at 1678 and 1624 cm^{-1} occur in the characteristic spectral range for asparagine side chains, the ν(C=O) mode contributing at 1678 cm^{-1} and the δ(NH$_2$) mode at 1624 cm^{-1}. On the basis of the structural data (*8*), no interactions between Tyr35 and a neighboring asparagine can be expected in the wild-type enzyme. However, upon mutation to Phe35, a different orientation of the residue toward Asn113 or Asn131 is well possible and would explain the IR difference signals.

In the spectral range between 1620 and 1590 cm^{-1}, smaller changes can be seen and tentatively attributed to the $\nu_{8a/8b}$-(CC) ring mode of Tyr35. At 1588 cm^{-1}, the decrease of a strong signal can be observed. The assignment of this difference band to a tyrosine mode is not probable because
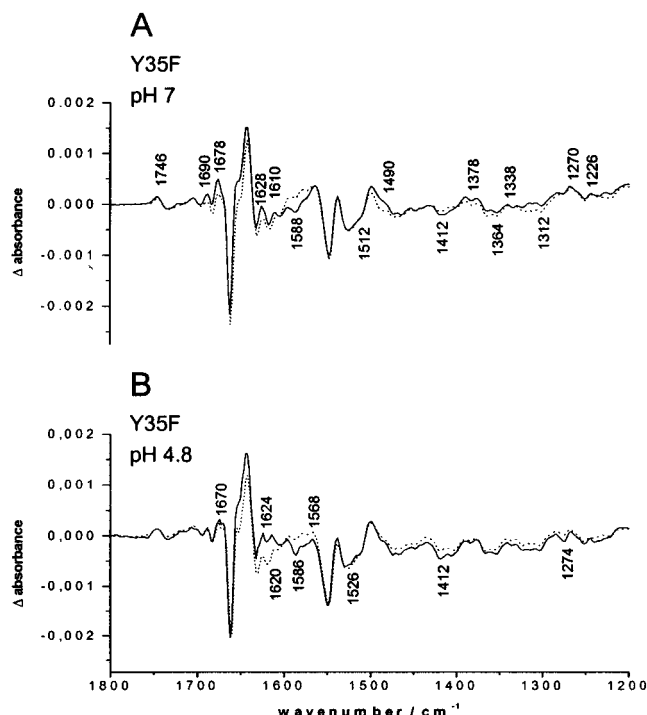
FIGURE 9: Oxidized-minus-reduced FTIR difference spectra of wild-type (dashed line) and Tyr35Phe mutant (full line) cytochrome *c* oxidase from *P. denitrificans* obtained for a potential step from −0.5 to 0.5 V (vs Ag/AgCl/3 M KCl) at pH 7 (A) and at pH 4.8 (B).

no signal of this intensity was shifted in the electrochemically induced FTIR difference spectra of the Tyr-D_4-labeled cytochrome *c* oxidase (Figure 2A). Ring modes from hemes *a* and a_3 as well as $\nu(COO^-)^{as}$ modes from aspartic acid or glutamic acid side chains are expected to contribute in this spectral range (for details, see ref *18*). However, it is not probable that these residues are affected upon mutation at this part of the protein. We thus tentatively assign the difference signal at 1588 cm^{-1} to an amide II mode, reflecting the perturbation of the polypeptide backbone upon exchange from Tyr35 to Phe35. Because amide groups orientate Tyr35, a perturbation of amide modes is conceivable (*8*). The shift of the mode at 1588 cm^{-1} upon H/D exchange, previously reported in Hellwig et al. (*16*), supports this assignment. For the variation at 1536 cm^{-1}, no explanation can be provided yet. The small variations at 1512 cm^{-1} can be attributed to the $\nu_{19}(CC)$ ring mode of the protonated tyrosine, reflecting the variations of the extinction coefficient based on changes in environment of the residue upon electron transfer and coupled proton translocation. This signal was also found for the Tyr-D_4-labeled cytochrome *c* oxidase (Figure 2A), thus supporting this assignment. At 1490 cm^{-1}, a signal develops that may be attributed to the $\nu(CC)$ ring mode of Phe35 on the basis of absorbance spectra of phenylalanine in solution (*39*). At lower wavenumbers, the increase of bands at 1412, 1384, and 1364 cm^{-1} and the shift of a band from 1336 to 1322 cm^{-1} can be seen. A possible assignment for these variations is the perturbation of the $\delta(COH)$ mode of serine side chains, expected between 1420 and 1248 cm^{-1} depending on their hydrogen bonding. Ser134 and Ser192 are located close to Tyr35 and are discussed as further residues involved in proton transfer along the D-pathway for protons (*5, 8*). The assignment of these modes to serine side chain,

however, needs confirmation by further mutagenesis experiments.

In the electrochemically induced FTIR difference spectra for pH 4.8, variations of a small mode at 1274, 1568, and 1624 cm^{-1} can be seen. These signals were also shifted in the spectra of the Tyr-D_4-labeled cytochrome *c* oxidase, allowing for the assignment of the shoulder at 1274 cm^{-1} in the double difference spectra wild-type minus Tyr-D_4-labeled oxidase (cf. Figure 3B) to the reorganization of the $\nu_{7'a}(CO)$ and $\delta(COH)$ mode of Tyr35. The absorption of the $\delta(COH)$ mode at 1274 cm^{-1} indicates the absence of strong hydrogen bonding; the presence of a rather weak hydrogen bonding to the phenolic group, however, cannot be excluded.

CONCLUSIONS

A difference signal at 1270/1268 cm^{-1} concomitant with the oxidized form was tentatively attributed to the composed $\nu_{7'a}(CO)$ and $\delta(COH)$ mode of Tyr280 and a signal at 1274 cm^{-1} assigned to Tyr35. These signals significantly increase for a pH step from 7 to 4.8. The change of the $\delta(COH)$ mode of Tyr35 at acidic pH is an important observation for the discussion of the protonation state of Tyr280. For both residues, a change of the intensity from this signal can be reported at pH 4.8. No uncommon absorptions can be expected for Tyr35, in contrast to the covalently linked Tyr280, and the lack of changes at modes sensitive to the protonation state at 1518/1500 cm^{-1} show that Tyr35 is protonated for the oxidized and reduced form. As a consequence, the possibility of a pH-dependent extinction coefficient of these modes needs to be taken into account and the variation of the signal at 1270 cm^{-1} in the Tyr280His mutant enzyme upon pH change does not necessarily describe a change of protonation state. The electrochemically induced FTIR difference spectra reflect the change of environment for Tyr280 upon electron transfer and a different environment at acid pH. The absorption of the $\delta(COH)$ mode at a relatively high frequency of 1270 cm^{-1} indicates the absence of hydrogen bonding to the phenol group of the tyrosine for Tyr35.

ACKNOWLEDGMENT

REFERENCES

1. Ferguson-Miller, S., and Babcock, G. T. (1996) *Chem Rev. 96*, 2889−2907.
2. Michel, H., Behr, J., Harrenga, A., and Kannt, A. (1998) *Annu. Rev. Biophys. Biomol. Struct. 27*, 329−356.
3. Hosler, J. P., Shapleigh, J. P., Mitchell, D. M., Kim, Y., Pressler, G. C., Babcock, G. T., Alben, J. O., Ferguson-Miller, S., and Gennis, R. B. (1996) *Biochemistry 35*, 10776−10783.
4. Ädelroth, P., Gennis, R. B., and Brzezinski, P. (1998) *Biochemistry 37*, 2470−2476.
5. Pfitzner, U., Odenwald, A., Ostermann, T., Weingard, L., Ludwig, B., and Richter, O.-M. H. (1998) *J. Bioenerg. Biomembr. 30*, 89−97.
6. Vygodina, T. V., Pecorano, C., Mitchell, D., Gennis, R., Konstantinov, A. A. (1998) *Biochemistry 37*, 3053−3061.
7. Zaslavsky, D., and Gennis, R. (1998) *Biochemistry 37*, 3062−3067.
8. Ostermeier, C., Harrenga, A., Ermler, U., and Michel, H. (1997) *Proc. Natl. Acad. Sci. U.S.A. 94*, 10547−10553
9. Gennis, R. B. (1998) *Biochim. Biophys. Acta 1365*, 241−248.

10. Michel, H. (1998) *Proc. Natl. Acad. Sci. U.S.A. 95*, 12819−12824.
11. Hoganson, C. W., Pressler, M. A., Proshlyakov, D. A., and Babcock, G. T. (1998) *Biochim. Biophys. Acta 1365*, 170−174.
12. Kannt, A., Lancaster, C. R. D., and Michel, H. (1998) *J. Bioenerg. Biomembr. 30*, 81−87.
13. Yoshikawa, S., Shinzawa-Itoh, K., Nakashima, R., Yaono, R., Yamashita, E., Inoue, N., Yao, M., Fei, M. J., Libeu, C. P., Mizushima, T., Yamaguchi, H., Tomizaki, T., and Tsukihara, T. (1998) *Science 280*, 1723−1729.
14. Buse, G., Soulimane, T., Dewor, M., Meyer, H. E., and Blüggel, M. (1999) *Protein Sci. 8*, 985−990.
15. Hellwig, P., Rost, B., Kaiser, U., Ostermeier, C., Michel, H., and Mäntele, W. (1996) *FEBS Lett. 385*, 53−57.
16. Hellwig, P., Behr, J., Ostermeier, C., Richter, O.-M. H., Pfitzner, U., Odenwald, A., Ludwig, B., Michel, H., and Mäntele, W (1998) *Biochemistry 37*, 7390−7399.
17. Behr, J., Hellwig, P., Mäntele, W., and Michel, H. (1998) *Biochemistry 37*, 7400−7406.
18. Hellwig, P., Grzybek, S., Behr, J., Ludwig, B., Michel, H., and Mäntele, W. (1999) *Biochemistry 38*, 1685−1694.
19. Kleymann, G., Ostermeier, C., Ludwig, B., Skerra, A., and Michel, H. (1995) *Biotechnology 13*, 155−160.
20. MacMillan, F., Kannt, A., Behr, J., Prisner, T., Michel, H. (1999) *Biochemistry 38*, 9179−9184.
21. Witt, H., Zickermann, V., and Ludwig, B. (1995) *Biochim. Biophys. Acta 1230*, 74−76.
22. Rost, B., Behr, J., Hellwig, P., Richter, O.-M. H., Ludwig, B., Michel, H., and Mäntele, W. (1999) *Biochemistry 38*, 7565−7571.
23. Kannt, A. (1999) Ph.D. Thesis, Frankfurt, Germany.
24. Moss, D. A., Nabedryk, E., Breton, J., and Mäntele, W. (1990) *Eur. J. Biochem. 187*, 565−572.
25. Venyaminov, S. Y., and Kalnin, N. N. (1990) *Biopolymers 30*, 1259−1271.
26. Hienerwadel, R., Boussac, A., Breton, J., Diner, B., and Berthomieu, C. (1997) *Biochemistry 36*, 14712−14723.
27. Thomas, J. W., Calhoun, M. W., Lemieux, L. J., Puustinen, A., Wikström, M., Alben, J. O., and Gennis, R. B. (1994) *Biochemistry 33*, 13013−13021.
28. Das, T. K., Pecoraro, C., Tomson, F. L., Gennis, R. B., and Rousseau, D. (1998) *Biochemistry 37*, 14471−14476.
29. Yamazaki, Y., Kandori, H., and Mogi, T. (1999) *J. Biochem. (Tokyo) 126*, 194−199.
30. Alben, J. O., Moh, P. P., Fiamingo, F. G., and Altschuld, R. A. (1981) *Proc. Natl. Acad. Sci. U.S.A. 78*, 234−237.
31. Fiamingo, F. G., Altschuld, R. A., and Alben, J. O. (1986) *J. Biol. Chem. 261*, 12976−12987.
32. Shapleigh, J. P., Hill, J. J., Alben, J. O., and Gennis, R. B. (1992) *J. Bacteriol. 174*, 2338−2343.
33. Nicholls, P., and Petersen, L. C. (1972) *Biochim. Biophys. Acta 357*, 462−467.
34. Wikström, M. K. F., Harmon, H. J., Ingledew, W. J., Chance, B. (1976) *FEBS Lett. 65*, 259−277.
35. Babcock, G. T., Vickery, L. E., and Palmer, G. (1978) *J. Biol. Chem. 7*, 2400−2411.
36. Wikström, M. K., Krab, K., and Saraste, M. (1981) *Cytochrome oxidase, A synthesis*, pp 1−198, Academic Press, New York.
37. Carter, K., and Palmer, G. (1982) *J. Biol. Chem. 257* (2), 13507−13514.
38. Hendler, R. W., and Westerhoff, H. V. (1992) *Biophys. J. 63*, 1586−1604.
39. Colthup, N. B., Daly, L. H., and Wiberley, S. E. (1990) *Introduction to Infrared and Raman Spectroscopy*, 3rd ed., Academic Press, New York.
40. Behr, J., Michel, H., Mäntele, W., and Hellwig, P. (2000) *Biochemistry 39*, 1356−1363.
41. McCauley, M. K., Vrtis, J. M., Dupont, J., and van der Donk, W. (2000) *J. Am. Chem. Soc. 10*, 2403−2404.

BI012056R